Title	The Separation mechanism of Am(III) from Eu(III) by diglycolamide and nitrilotriacetamide extraction reagents using DFT calculations
Author(s)	Masashi Kaneko, Masayuki Watanabe and Tatsuro Matsumura
Citation	Dalton Transactions, 45(43), p.17530-17537
Text Version	Publisher
URL	http://jolissrch-inter.tokai-sc.jaea.go.jp/search/servlet/search?5056894
DOI	http://dx.doi.org/10.1039/C6DT03002E
Right	

Dalton Transactions

PAPER

View Article Online
View Journal | View Issue

Cite this: *Dalton Trans.*, 2016, **45**, 17530

The separation mechanism of Am(III) from Eu(III) by diglycolamide and nitrilotriacetamide extraction reagents using DFT calculations†

Masashi Kaneko, Masayuki Watanabe* and Tatsuro Matsumura

Received 29th July 2016,
Accepted 5th October 2016

DOI: 10.1039/c6dt03002e

www.rsc.org/dalton

Relativistic density functional calculations were applied to study the separation behaviors of the Am(III) ion from the Eu(III) ion by diglycolamide (DGA) and nitrilotriacetamide (NTA) ligands in order to understand the difference in the separation mechanism of their reagents. The complexation reaction was modeled on the basis of previous experimental studies. The calculated energies based on stabilization by complex formation at the ZORA-B2PLYP/SARC level predicted that the DGA reagent preferably coordinated to the Eu(III) ion when compared with the Am(III) ion. In contrast, the NTA reagent selectively coordinated to the Am(III) ion when compared with the Eu(III) ion. These results reproduced the experimental selectivity of DGA and NTA ligands toward Eu(III) and Am(III) ions. Mulliken's population analyses implied that the difference in the contribution of the bonding property between the f-orbital of Am and donor atoms determined the comparative stability of Eu and Am complexes.

Introduction

High-level radioactive waste (HLLW) is generated during the reprocessing of spent nuclear fuel and contains minor actinide (MA = Np, Am, Cm) ions. The partitioning and transmutation (P & T) technology, which involves the transmutation of MA nuclides to short-lived or non-radioactive nuclides following the selective partitioning of MA ions, was developed over several decades because of the radiotoxicity of MA nuclides (possessing long-lived radioactivity and α-active nuclides).[1] A crucial difficulty in achieving MA partitioning involves the separation between MA ions and lanthanide (Ln) ions in HLLW. This is because Ln ions are also contained in HLLW as fission products and show similar chemical properties to MA ions, such as the oxidation state, ionic radii, and geometries of metal complexes in aqueous solution.[2] Hence, it is desirable to develop separation techniques and to investigate the separation mechanism of MA from Ln.

N,*N*,*N*′,*N*′-Tetraalkyl diglycolamide (TRDGA)[3] and *N*,*N*,*N*′,*N*′,*N*,″*N*″-hexaalkyl nitrilotriacetamide (HRNTA)[4] reagents were investigated as candidates for the separation between MA and Ln ions by using the solvent extraction method (Fig. 1).

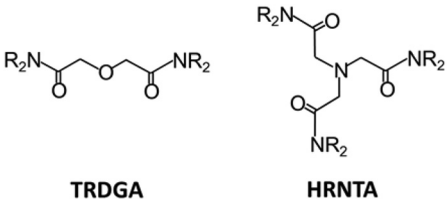

Fig. 1 Molecular structures of TRDGA and HRNTA ligands.

Specifically, the hexaoctyl-NTA (HONTA) ligand displays selectivity for MA ions over Ln ions, D_{Am}/D_{Eu} = 52.6,‡ because a nitrogen atom as a soft-donor seems to have the suitable donor ability to the Am ion.[4] Conversely, tetraoctyl-DGA (TODGA) exhibits reverse selectivity for an Am/Eu system, D_{Am}/D_{Eu} = 0.113,‡ when compared with that of the HONTA system.[3] Although understanding the difference in the separation mechanisms of MA from Ln between the TRDGA and HRNTA ligands is desired for the molecular design of the extraction ligands with higher selectivity toward MA ions, this difference has not been investigated in previous studies.

Density functional theory (DFT) calculation is a powerful tool to understand the electronic state of f-block compounds.

Nuclear Science and Engineering Center, Japan Atomic Energy Agency, Japan. E-mail: watanabe.masayuki@jaea.go.jp

† Electronic supplementary information (ESI) available: Cartesian coordinates of calculated geometries as xyz file formats, total energies of all compounds, and data of orbital energies with PDOS and MOOP for $[M(TMDGA)_3]^{3+}$ and $[M(HMNTA)(H_2O)_5]^{3+}$ (M = Eu, Am). See DOI: 10.1039/c6dt03002e

‡ The value of D_{Am}/D_{Eu} = 52.6 was obtained from ref. 4*a* under the condition of 0.2 M HNO_3 with 0.5 M HONTA/*n*-dodecane. The value of D_{Am}/D_{Eu} = 0.113 was obtained from ref. 3*a* under the condition of 1 M HNO_3 with 0.1 M TODGA/*n*-dodecane.

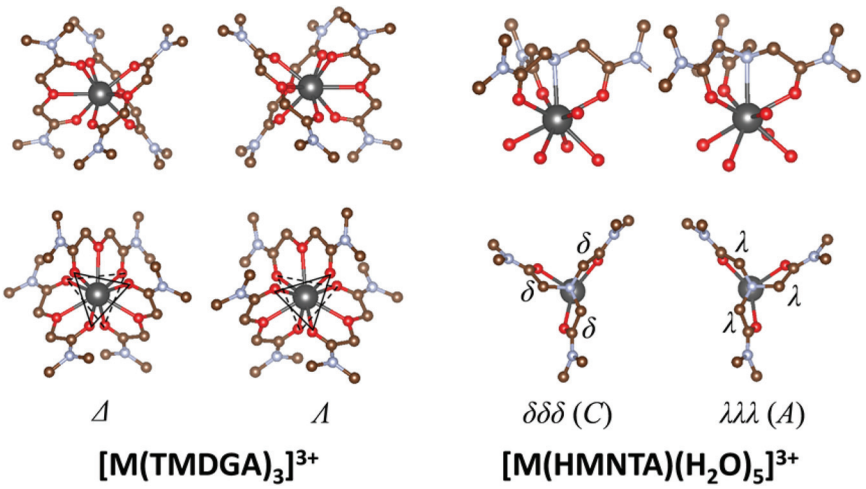

Fig. 2 Ball-and-stick description of coordination geometries for $[M(TMDGA)_3]^{3+}$ and $[M(HMNTA)(H_2O)_5]^{3+}$ complexes. The black, red, blue, and brown spheres represent metal, oxygen, nitrogen, and carbon atoms, respectively. Hydrogen atoms are omitted for clarity.

There are many previous studies focusing on the chemical stability and bonding properties of f-block complexes using DFT calculation.[5] Recently, increasing research attention has focused on the separation between MA and Ln ions using DFT calculation[6] and extant studies indicate that the stabilization of metal ions by complexation in aqueous solutions is required to reproduce the experimental separation behaviors.[7] Additionally, a previous study suggested that the difference in the bonding contribution of valence f-electrons was related to the selectivity of Am from Eu.[8]

The aim of this study involved applying DFT calculation to study the separation behavior of Am from Eu using TRDGA and HRNTA extraction ligands and interpreting the separation mechanism from the bonding viewpoint. In this study, the modeling of the molecular structures and the complexation reaction for Am/Eu ions with TRDGA and HRNTA ligands was demonstrated in accordance with the methods proposed by extant research. The correlation between the bonding properties and the separation behavior of Am/Eu with TRDGA and HRNTA ligands was discussed by means of Mulliken's population analyses after validating the reproducibility of the experimental selectivity for Am/Eu ions. The separation mechanism for these systems involved the construction of the fundamental chemistry for the separation of f-block ions as well as their application in the P & T process.

Computational details

Solvent extraction studies revealed the molecular composition of the extraction complexes using DGA and NTA ligands. In the case of the DGA system, three equivalents of DGA ligands coordinated to one MA^{III}/Ln^{III} ion.[3] Single crystal structural investigations were conducted for several types of Ln^{III} ions with tetraethyl-DGA ligands,[9a] and recently for the Am^{III} ion[9b] with tetramethyl-DGA ligands. It was reported that the chemical component ratio of metal : ligand for DGA complexes was 1 : 3 and each DGA ligand worked as a tridentate chelate.[9] In the case of the NTA system, the ratio of ligand to metal was 1 for Ln^{III} and 1 or 2 for MA^{III}.[4] Single crystal structures for [M(hexabutyl-NTA)(pic)$_3$] (M = Eu^{III}, Tb^{III}; Hpic = picric acid) revealed that the NTA ligand coordinated to the metal ion as a tetra-dentate donor and that the five oxygen donors filled the coordination space.[10] Both the DGA and NTA systems included two conformers, namely, Δ and Λ conformers, in the case of the DGA system and $\delta\delta\delta$ (clockwise; C) and $\lambda\lambda\lambda$ (anti-clockwise; A) conformers in the case of the NTA system (Fig. 2). The molecular structures of DGA and NTA complexes were considered as $[M(TMDGA)_3]^{3+}$ and $[M(HMTNA)(H_2O)_5]^{3+}$ (M = Eu^{III}, Am^{III}; TMDGA = tetramethyl-DGA; HMNTA = hexamethyl-NTA), respectively. In order to reduce the computational costs, all alkyl chains bonded to the amide nitrogen atom of DGA and NTA were replaced by methyl groups. We think that this approximation is valid, because the separation behavior of Am from Eu using a DGA-type ligand did not depend on the lengths of alkyl chains for DGA.[3a] Three pic donors in [M(hexabutyl-NTA)(pic)$_3$] were substituted by five water molecules to examine the coordination structure in aqueous solution. The molecular geometries of $[M(TMDGA)_3]^{3+}$, including Δ and Λ conformers, were modeled by referring to the CCSD codes, namely, LOCFAM and LUVPOJ for M = Eu^{III} and Am^{III}, respectively. The geometries of $[M(HMTNA)(H_2O)_5]^{3+}$, including the $\delta\delta\delta$ and $\lambda\lambda\lambda$ conformers, were modeled by referring to the CCSD code CIRTAZ for both M = Eu and Am systems since the Am complex with the NTA ligand was not available. However, the replacement of Eu with Am was considered as a suitable treatment because generally Am^{III} complexes have crystal structures and coordination spheres that are similar to Ln^{III} complexes.[11]

The computational models for the complexation scheme involved the stabilization reaction toward a nona-hydrated

complex, $[M(H_2O)_9]^{3+}$ by replacing H_2O molecules with DGA or NTA ligands, as shown in eqn (1) and (2) given below:

$$[M(H_2O)_9]^{3+} + 3TMDGA \rightarrow [M(TMDGA)_3]^{3+} + 9H_2O \quad (1)$$

$$[M(H_2O)_9]^{3+} + HMNTA \rightarrow [M(HMNTA)(H_2O)_5]^{3+} + 4H_2O \quad (2)$$

The Gibbs energy difference (ΔG) for the complexation reaction was obtained as the energy difference in the sum of the Gibbs energy values between the reactants and products in eqn (3). The Gibbs energy was divided into total energy (E^{tot}) and a thermal Gibbs correction term (G^{corr}) shown in eqn (4). The G^{corr} term includes a thermal correction for enthalpy (H^{corr}) and an entropy term (S), as shown in eqn (5). The H^{corr} and S terms include the contributions from vibration, rotation, and translation, as shown in eqn (6) and (7). k_B and T denote the Boltzmann constant and the temperature, respectively.

$$\Delta G = G(\text{product}) - G(\text{reactant}) \quad (3)$$

$$G = E^{tot} + G^{corr} \quad (4)$$

$$G^{corr} = H^{corr} - TS \quad (5)$$

$$H^{corr} = U^{vibration} + U^{rotation} + U^{translation} + k_B T \quad (6)$$

$$S = S^{spin} + S^{vibration} + S^{rotation} + S^{translation} \quad (7)$$

The selectivity of DGA or NTA ligands toward Am/Eu ions was evaluated by comparing the ΔG values between the Am and Eu systems.

All relativistic DFT calculations were performed using the ORCA ver. 3.0.0 program[12] with a zero-order regular approximation (ZORA).[13] The scalar relativistic effect was considered by a spin-free ZORA Hamiltonian using Wüllen's procedure,[14] to which a Breit–Pauli spin–orbit coupling formalism was perturbatively added. Segmented all-electron relativistically contracted (SARC) basis sets for ZORA were assigned to all the atoms.[15]§ A spin-unrestricted Kohn–Sham equation was employed for open-shell system compounds. Geometry optimization steps were calculated using the quasi-Newton method at the BP86 level any geometrical constraints, given that the pure density functional with all-electron basis sets reproduced the experimental molecular geometries for the f-block compounds.[5b] Single-point energies were calculated at the B2PLYP functional with the TZVP basis set for O, N, C, and H atoms since the B2PLYP functional exhibited a good performance with respect to the experimental separation behaviors[8] and bonding properties for f-block complexes.[16] The spin multiplets for both Am^{III} and Eu^{III} complexes were regarded as septet states. The hydration effect by a bulk solvent was implicitly considered for a single-point calculation by using a conductor-like screening model (COSMO), in which COSMO radii of Am and Eu ions were assigned as 1.99 and 1.90 Å, respectively.[17] Split-RI-J and RIJCOSX approximations were employed in pure- and hybrid-DFT calculations.[18] All self-consistent field calculations were achieved within the same accuracy as the one shown in a previous study.[8]¶ Atomic spin population and bond overlap population analyses were calculated by Mulliken's procedure.[19] Three-dimensional descriptions of the optimized structures and molecular orbitals were visualized using the VESTA ver. 3.3.0 program.[20]

Results and discussion

Geometry optimization

All equilibrium structures optimized at the BP86/SV-ZORA level were obtained in local minimum geometries. Fig. 2 shows the obtained coordination structures of $[M(TMDGA)_3]^{3+}$ and $[M(HMNTA)(H_2O)_5]^{3+}$ complexes. The $[M(TMDGA)_3]$ geometry displayed a pseudo tricapped trigonal structure with the ether oxygen of TMDGA as a cap and the C_3 rotational axis along the perpendicular direction toward the plane, which included three oxygens of ether for both Δ and Λ conformers. The $[M(HMNTA)(H_2O)_5]^{3+}$ geometries, for both clockwise (C) and anti-clockwise (A) systems, revealed that the configuration of eight oxygen atoms had a distorted square antiprism structure. The coordination environments for C and A systems were almost identical except for the twisting direction of the amide group.

Table 1 shows the metal–ligand lengths of the DGA and NTA complexes. The M–O(CO) bond distances were consistent when the metal–ligand lengths of the DGA complexes, obtained in the calculation and the experiment, were compared. This bond length was in agreement with an experimental result (2.40(1) Å) in solution using EXAFS.[21] Although the calculated M–O(ether) lengths were longer than the experimental values by *ca.* 0.12 Å, this was not considered as important in the context of this study because the calculated structure maintained the molecular symmetry of the experimental X-ray geometry. Additionally, the previous computational report estimated the bond lengths between the Eu ion and ether oxygens of TODGA as 2.56–2.65 Å, which was consistent with the calculated bond lengths.[22] A comparison of the calculated bond lengths between the Eu and Am complexes indicated that both the structures were obtained with almost identical bond distances and geometrical environments. The calculated bond lengths between the Eu atom and the NTA ligand were in agreement with the experimental values for both C and A conformers when compared with the metal–ligand

§ SV-ZORA with one polarization and TZV-ZORA with one polarization were assigned to C, N, O and H atoms for geometry optimization and single-point calculation, respectively.[15a] The SARC basis set was assigned to Eu ($61^{17}/51^{11}/41^{8}/41^{2}$)[15b] and Am ($91^{20}/81^{12}/71^{9}/61^{6}$)[15c] for both geometry optimization and single-point calculation.

¶ Angular grid points in self-consistent field (SCF) calculations are set to Lebedev194 for optimization with no final grid calculation and Lebedev302/Lebedev434 for single-point calculation (iteration/final grid). Integral accuracy parameters are set to 4.34 for optimization and 4.67/5.01 for single-point calculation where the special grid is additionally constructed for Eu and Am atoms with an integral accuracy of 14.0 in order to improve the precision of SCF energies. All SCF calculations are achieved under the generally tight condition imposing a threshold value of 10^{-8} hartree to total energy difference during iteration.

Table 1 Metal–ligand bond lengths with standard deviations shown in parentheses for calculated and experimental complexes for DGA and NTA systems (Å)

		M = Eu		M = Am	
Compounds	Bond	Calc.	Exp.[9a]	Calc.	Exp.[9b]
$M(DGA)_3$ (Δ)	M–O(CO)	2.421(12)	2.389(14)	2.445(18)	2.459(21)
	M–O(ether)	2.617(5)	2.489(15)	2.644(1)	2.519(8)
$M(DGA)_3$ (Λ)	M–O(CO)	2.421(12)	2.408(22)	2.510(18)	2.459(21)
	M–O(ether)	2.617(5)	2.480(12)	2.643(6)	2.519(8)
$M(NTA)(H_2O)_5$ (C)	M–N(NTA)	2.771	2.770	2.723	—
	M–O(NTA)	2.384(31)	2.404(37)	2.394(34)	—
	M–O(H_2O)	2.578(82)	—	2.610(90)	—
$M(NTA)(H_2O)_5$ (A)	M–N(NTA)	2.787	2.742	2.725	—
	M–O(NTA)	2.401(38)	2.387(31)	2.429(33)	—
	M–O(H_2O)	2.552(22)	—	2.567(44)	—

lengths of NTA complexes. A comparison of the calculated lengths between Eu and Am complexes indicated that Eu and Am complexes have similar geometries as in the case of DGA complexes.

Energy analysis

In the analysis, $\Delta\Delta G$ was defined in terms of eqn (8). Hence, a negative $\Delta\Delta G$ implied that the Eu complex was more stable than the Am complex when compared with their corresponding hydrated complexes, while a positive $\Delta\Delta G$ suggested that the Am complex was more stable.

$$\begin{aligned}\Delta\Delta G &= \Delta G(\mathrm{Eu}) - \Delta G(\mathrm{Am}) \\ &= [\Delta E^{\mathrm{tot}}(\mathrm{Eu}) + \Delta G^{\mathrm{corr}}(\mathrm{Eu})] - [\Delta E^{\mathrm{tot}}(\mathrm{Am}) + \Delta G^{\mathrm{corr}}(\mathrm{Am})] \\ &= [\Delta E^{\mathrm{tot}}(\mathrm{Eu}) - \Delta E^{\mathrm{tot}}(\mathrm{Am})] + [\Delta G^{\mathrm{corr}}(\mathrm{Eu}) - \Delta G^{\mathrm{corr}}(\mathrm{Am})] \\ &= \Delta\Delta E^{\mathrm{tot}} + \Delta\Delta G^{\mathrm{corr}}\end{aligned} \quad (8)$$

The total energy difference, $\Delta E^{\mathrm{tot}}(\mathrm{M})$, *via* the B2PLYP method and the difference of the Gibbs thermal correction energy, $\Delta G^{\mathrm{corr}}(\mathrm{M})$, calculated using the BP86 method were based on the normal vibrational analysis at 298.15 K. As shown in Table 2, in the case of the DGA system, ΔG(Eu) was smaller than ΔG(Am). In contrast, in the case of the NTA system, ΔG(Eu) was almost the same as or slightly larger than ΔG(Am). This indicated that the TMDGA ligand preferably coordinated to the Eu^{III} ion when compared with the Am^{III} ion, whereas the HMNTA ligand preferably coordinated to the Am^{III} ion. This tendency was consistent with the experimental selectivity of Am ions when compared with Eu ions using TODGA[3a] and HONTA[4] ligands. The contribution of ΔE^{tot} and ΔG^{corr} to $\Delta\Delta G$ was compared between the DGA and NTA systems. The comparison indicated that the $\Delta\Delta E^{\mathrm{tot}}$ value changed from $[M(TMDGA)_3]^{3+}$ to $[M(HMNTA)(H_2O)_5]^{3+}$ by *ca.* 9 kJ mol^{-1}. However, the change in $\Delta\Delta G^{\mathrm{corr}}$ was small (~2 kJ mol^{-1}), indicating that $\Delta\Delta G$ was contributed by mainly $\Delta\Delta E^{\mathrm{tot}}$ and not $\Delta\Delta G^{\mathrm{corr}}$. Thus, it was suggested that the major factor that determined the selectivity of Am to Eu was the electronic and not the geometrical contribution since the $\Delta\Delta G^{\mathrm{corr}}$ term depended on the structural difference between Eu and Am complexes, and there were no significant differences as mentioned above. Recently, a computational study has been reported for the DGA system. Narbutt *et al.*[22b] and Ali *et al.*[22c] indicated that the DGA ligand preferentially coordinates to the Eu ion compared to the Am ion, as well as our result. However, Wang *et al.* suggested that the Am–DGA complex formed is more stable than the Eu–DGA complex.[22a] These different results might attribute to the difference of the complex models, $[M(DGA)(NO_3)_3]$[22a] and $[M(DGA)_3]$.[22b,c] In this study, we focused on the stability of the $[M(DGA)_3]$ complex.

Table 3 shows the comparison of $\Delta\Delta E^{\mathrm{tot}}$ values for the DGA and NTA systems using three density functionals, namely, BP86, B3LYP, and B2PLYP. In the case of the DGA system, the $\Delta\Delta E^{\mathrm{tot}}$ value was negative for all the methods. However, in the case of the NTA system, the $\Delta\Delta E^{\mathrm{tot}}$ value increased significantly in the respective order of BP86, B3LYP, and B2PLYP methods by 12.8 kJ mol^{-1} when compared with 6.7 kJ mol^{-1} in

Table 2 ΔG(M) and $\Delta\Delta G$ values based on ΔE^{tot}(M) at B2PLYP and ΔG^{corr}(M) at BP86

Energy	$[M(TMDGA)_3]$ (Δ/Λ)	$[M(HMNTA)(H_2O)_5]$ (C/A)
ΔG(Eu)/kJ mol^{-1}	−402.9/−398.3	−209.1/−219.3
ΔG(Am)/kJ mol^{-1}	−391.1/−395.9	−208.3/−223.5
$\Delta\Delta G$/kJ mol^{-1}	−7.1	+1.7
$\Delta\Delta E^{\mathrm{tot}}$/kJ mol^{-1}	−2.7	+4.1
$\Delta\Delta G^{\mathrm{corr}}$/kJ mol^{-1}	−4.4	−2.4
$\Delta\Delta G^{\mathrm{exp}}$/kJ mol^{-1}	−5.4[a]	+9.8[a]

[a] Calculated by using $\Delta\Delta G = RT\ln(D_{\mathrm{Am}}/D_{\mathrm{Eu}})$ at 298.15 K based on the separation factors of 0.113[‡] and 52.6[‡] for DGA and NTA complexes, respectively.

Table 3 A comparison of $\Delta\Delta E^{\mathrm{tot}}$ among BP86, B3LYP, and B2PLYP methods

	$\Delta\Delta E^{\mathrm{tot}}$/kJ mol^{-1}	
Method	$[M(TMDGA)_3]$	$[M(HMNTA)(H_2O)_5]$
BP86	−9.4	−8.7
B3LYP	−4.6	−0.2
B2PLYP	−2.7	+4.1

the case of the DGA system. As indicated by the previous calculations using dithiophosphinic acid, *N*,*N*,*N*′,*N*′-tetrakis(2-pyridylmethyl)-ethylenediamine, and phosphinic acid as ligands, the B2PLYP method reproduced the experimental separation behavior of the Am ions from Eu ions by DGA and NTA ligands when compared to those of the BP86 and B3LYP methods.[8] It was considered that the selectivity between the Am and Eu ions depended on the exact exchange admixture included in each functional because the bonding contribution of the f-electron was influenced by the evaluation of exchange interactions between the electrons. The results also indicated that the mixing ratio of 53% in the B2PLYP functional was suitable for describing the separation behavior of Am from Eu when compared to the mixing ratios of 0% in the BP86 functional and 20% in the B3LYP functional.

Population analysis

Table 4 shows the spin population values (ρ_{spin}) of the metal atom for the DGA and NTA complexes obtained using Mulliken's method. We also show the results of Löwdin's spin population[23] for the comparison with Mulliken's method because Mulliken's procedure depends on employing basis sets. The electron–electron interaction between the metal and ligands grows stronger with increase in the difference between ρ_{spin} and 6.0. The ρ_{spin} values obtained *via* the BP86 method were quite large, especially for Eu complexes, when compared with those of the other methods. This indicated that the BP86 method overestimated the covalent interaction between the Eu atom and the TMDGA and the HMNTA ligands, leading to the wrong evaluation of the selectivity of NTA between the Eu and Am ions, as shown in Table 3. A comparison of the ρ_{spin} values *via* the B2PLYP method showed that the ρ_{spin} value of the Am complex increased from the DGA to the NTA system by 0.017 electrons for Mulliken's method and 0.013 electrons for Löwdin's method. In contrast, the ρ_{spin} value of the Eu complex increased from the DGA to the NTA system by *ca*. 0.010 electrons. This implied that the slight difference in the ρ_{spin} values for both Mulliken's and Löwdin's methods influenced the bonding property in the DGA and the NTA complexes. Table 5 shows the bond order values between the metal and ligands by Mayer's method[24] and indicates that in the case of the DGA complex, the Eu–O bond is stronger than the Am–O bond, whereas in the case of the NTA complex, the Am–N bond is stronger than the Eu–N bond. It was suggested that the covalency between the metal and ligands correlates with the selectivity in Am/Eu ions by ligands. Recently, there has been an interesting study performing the extraction experiments using the *N*-pivot tripodal DGA extractant (DGA-TREN), which has an analogous structure to the NTA ligand.[25] The DGA-TREN ligand did not show the selectivity toward the Am ion, because it was predicted that the nitrogen element did not work as a donor atom using the EXAFS experiment and DFT calculation.[25] This indicated that in order to gain the selectivity toward the Am ion, the N-donor needs to coordinate to a metal ion as the NTA ligand.

Table 5 Mayer's bond order values of the metal–ligand bond in DGA and NTA complexes at B2PLYP

Compounds	Bond	M = Eu	M = Am
$[M(DGA)_3]$ (Δ)	M–O(CO)	0.174	0.149
$[M(DGA)_3]$ (Λ)	M–O(CO)	0.173	0.148
$[M(NTA)(H_2O)_5]$ (C)	M–N(NTA)	0.131	0.142
	M–O(NTA)	0.220	0.210
$[M(NTA)(H_2O)_5]$ (A)	M–N(NTA)	0.129	0.145
	M–O(NTA)	0.204	0.198

Mulliken's bond overlap population, which shows the strength and the sign of the bond overlap between basis functions, was calculated.[19] Recently, this analysis was employed in computational studies involving the separation of MA ions; moreover, it provided useful information regarding the bonding properties of f-block compounds.[8,26] The bond overlap population of the *i*th MO, termed OP^i, can be described in terms of eqn (9) as follows:

$$OP^i = 2\Sigma_\mu \Sigma_\nu c_\mu{}^i c_\nu{}^i S_{\mu\nu} \quad (9)$$

where c_μ and c_ν denote the MO coefficients toward basis functions χ_μ and χ_ν, respectively, and $S_{\mu\nu}$ denotes the overlap integral between χ_μ and χ_ν. In order to discuss the bonding property between the f-orbital of the metal atom and donor atoms, μ was defined as belonging to a set of f-type basis functions in a metal atom and ν was defined as belonging to the set of all basis functions in the donor atoms. Fig. 3 shows the partial densities of states (PDOS) of the f-orbital in the metal atom and OP in the valence region, which was described as a Gaussian line convoluted with a half-width of 0.5 eV for

Table 4 Mulliken's and Löwdin's spin populations (ρ_{spin}) of the metal atom in DGA and NTA complexes

	ρ_{spin} of metal atom/electron			
	$[M(TMDGA)_3]$ (Δ/Λ)		$[M(HMNTA)(H_2O)_5]$ (C/A)	
Method	M = Eu	M = Am	M = Eu	M = Am
BP86 (Mulliken)	6.201/6.199	6.057/6.053	6.249/6.251	6.094/6.093
B3LYP (Mulliken)	6.046/6.041	6.015/6.013	6.067/6.069	6.037/6.036
B2PLYP (Mulliken)	6.041/6.033	6.025/6.025	6.045/6.048	6.042/6.042
BP86 (Löwdin)	6.183/6.183	6.012/6.012	6.229/6.231	6.045/6.044
B3LYP (Löwdin)	6.040/6.036	5.996/5.994	6.059/6.062	6.016/6.015
B2PLYP (Löwdin)	6.033/6.027	6.007/6.007	6.037/6.039	6.020/6.021

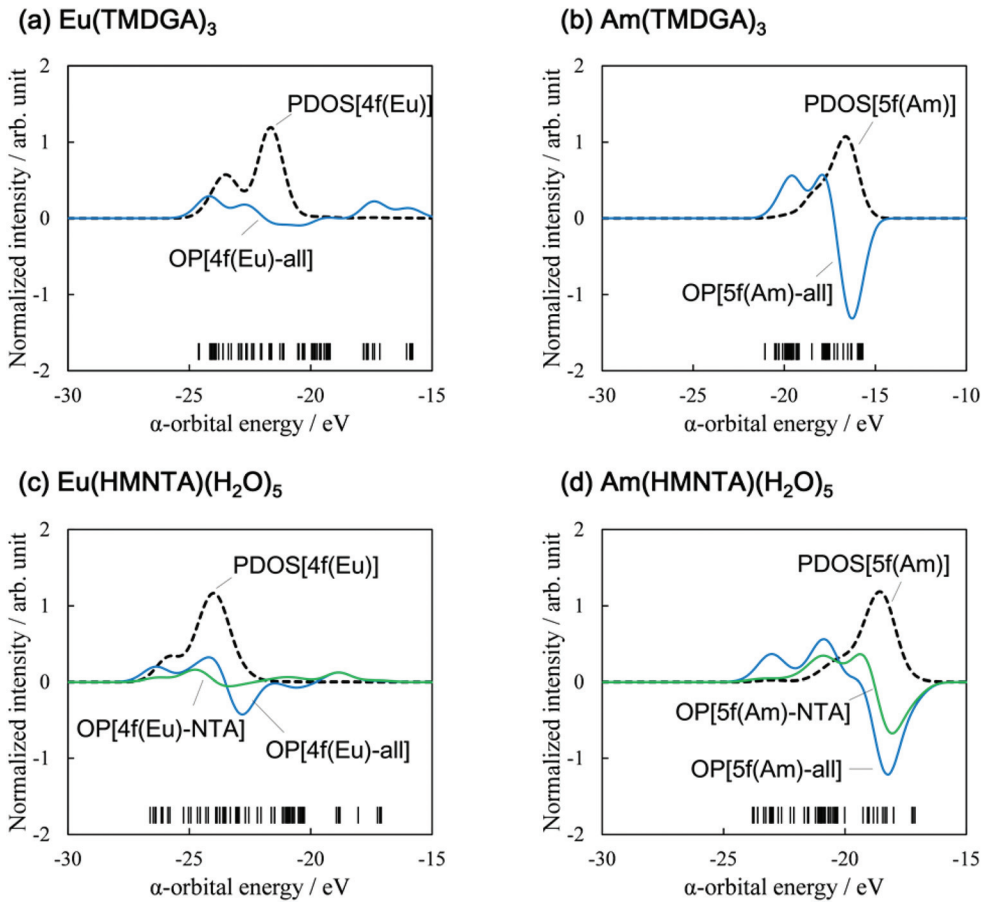

Fig. 3 Partial densities of states (PDOS) curves of f-orbital electrons (black dashed lines) and bond overlap population (OP) curves between f-orbital electrons and donor atoms of all ligands (blue solid lines) and the NTA ligand (green solid lines) for $[M(TMDGA)_3]^{3+}$ (M = (a) Eu, (b) Am) and $[M(HMNTA)(H_2O)_5]^{3+}$ (M = (c) Eu, (d) Am) in the valence α-orbital region. All lines were described in terms of a Gaussian line convoluted with a half-width value of 0.5 eV.

$[M(TMDGA)_3]^{3+}$ (*Δ*) and $[M(HMNTA)(H_2O)_5]^{3+}$ (A) *via* the B2PLYP method. By focusing on the OP curve in the region where PDOS was distributed, it was observed that the contribution of the positive OP was indicated for Eu complexes in both the DGA and NTA systems. Conversely, a large negative OP was found for Am complexes. This indicated that the 4f-orbital of the Eu atom contributed to a weak bonding interaction, whereas the 5f-orbital of the Am atom participated in a strong anti-bonding interaction. When the 5f-orbital contributions of the Am atom between the DGA and NTA complexes were compared, it was revealed that the anti-bonding contribution of the NTA complex was weakened by the comparatively positive contribution of the overlap with the NTA ligand when compared to those present in the DGA system.

Based on the MO analyses in Fig. 3, the orbital diagram of f-type MOs is split into bonding type and anti-bonding type MOs as shown in Fig. 4. By comparing the proportion of the f-orbital contribution in the metal atom, it was observed that the bonding contribution of the NTA complex was higher than that of the DGA complex for both Eu and Am systems. The sum of normalized OP, which was regarded as the OP between the f-orbital of the metal atom and donor atoms of a DGA/NTA ligand, was calculated and shown in parentheses (Fig. 4). The change in the absolute values of the OP sum between the DGA and NTA complexes was small in the case of the Eu system and large in the case of the Am system. This indicated that the small bond overlapping in the Eu–DGA/NTA bond does not influence the ρ_{spin} as shown in Table 4, on the other hand, the large bond overlapping in the Am–DGA/NTA bond offers a significant effect to the spin population. Focusing on the covalency in Am complexes, in the case of the DGA system the accumulation of electrons in molecular orbitals with large anti-bonding overlapping weakens the Am–DGA bond. As a result, the Eu–DGA complex had the larger Mayer bond order. Whereas in the Am–NTA system due to the electron occupation in MOs with more bonding-type overlapping compared to the Am–DGA system, the Am–N bond was stronger than the Eu–N bond. It was suggested that this different behavior in the metal–ligand covalent interaction might be attributed to the chemical stability of these complexes. It is necessary to carefully investigate the correlation between the stability of each complex and the covalency of f-orbital electrons in future studies. However, it is expected that the difference in the bond overlapping of the f-orbital in the metal atom with donor

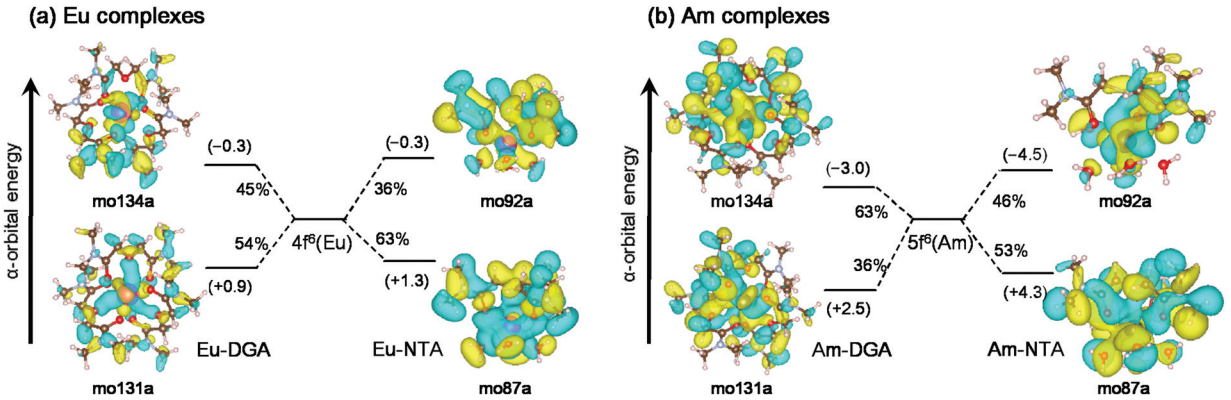

Fig. 4 An f-type MO diagram divided into bonding and anti-bonding orbitals for (a) Eu and (b) Am complexes based on bond overlap population analyses. The values in parentheses represent the sum of normalized OP through each region. Isosurface descriptions of selected MOs were visualized at 2.5×10^{-5} electrons per bohr^3.

atoms could originate in the selectivity in Am and Eu ions by the DGA and NTA ligands.

Conclusions

In this study, the chemical separation of Am^{III} from Eu^{III} was demonstrated using DGA and NTA ligands by means of relativistic DFT calculations. The separation mechanism of Am from Eu was modeled as a complexation reaction in aqueous solution in accordance with experimental methods used in previous studies. The energy analysis based on the Gibbs energy under a water phase *via* the B2PLYP method reproduced the experimental selectivity of Am from Eu ions using the DGA and NTA ligands. Mayer's bond order indicated that the bond strength of Am–N in the NTA complex is stronger than that of Eu–N, leading to the stability of the Am–NTA complex than the Eu–NTA complex. Mulliken's population analyses revealed that the bond overlaps between the f-orbital of the Am atom and the NTA system displayed a stronger bonding contribution than that of the Am–DGA system, on the other hand, the strong anti-bonding contribution was observed in the Am–DGA system. This could be attributed to the difference in the experimental selectivity of the Am ion, elaborating the separation mechanisms of the DGA and NTA ligands. Additionally, the results of the study indicated the possibility that controlling the covalency of f-orbital electrons leads to the theoretical modeling of novel and effective separation materials of MA ions from Ln ions. This study contributes to the bonding theory in the field of f-block coordination chemistry as well as to the application of computational chemical studies in the disposal of HLLW.

Notes and references

1 H. Oigawa, K. Nishihara, S. Nakayama and Y. Morita, Proceedings of 10th Information Exchange Meeting, Mito, Japan, OECD/NEA, Paris, 2010.
2 K. L. Nash, *Solvent Extr. Ion Exch.*, 1993, **11**, 729.
3 (*a*) Y. Sasaki, Y. Sugo, S. Suzuki and S. Tachimori, *Solvent Extr. Ion Exch.*, 2001, **19**, 91; (*b*) Y. Sasaki, Z. Zhu, Y. Sugo and T. Kimura, *J. Nucl. Sci. Technol.*, 2007, **44**, 405; (*c*) S. A. Ansari, P. N. Pathak, P. K. Mohapatra and V. K. Manchanda, *Chem. Rev.*, 2012, **112**, 1751.
4 (*a*) Y. Sasaki, Y. Tsubata, Y. Kitatsuji and Y. Morita, *Chem. Lett.*, 2013, **42**, 91; (*b*) Y. Sasaki, Y. Tsubata, Y. Kitatsuji, Y. Sugo, N. Shirasu and Y. Morita, *Solvent Extr. Ion Exch.*, 2014, **32**, 179.
5 (*a*) N. Kaltsoyannis, *Chem. Soc. Rev.*, 2003, **32**, 9; (*b*) G. Schreckenbach and G. A. Shamov, *Acc. Chem. Res.*, 2010, **43**, 19; (*c*) C. Platas-Iglesias, A. Roca-Sabio, M. Regueiro-Figueroa, D. Esteban-Gomez, A. de Blas and T. Rodríguez-Blas, *Curr. Inorg. Chem.*, 2011, **1**, 91; (*d*) D. Wang, W. F. van Gunsteren and Z. Chai, *Chem. Soc. Rev.*, 2012, **41**, 5836.
6 J. Lan, W. Shi, L. Yuan, J. Li, Y. Zhao and Z. Chai, *Coord. Chem. Rev.*, 2012, **256**, 1406.
7 (*a*) X. Cao, D. Heidelberg, J. Ciupka and M. Dolg, *Inorg. Chem.*, 2010, **49**, 10307; (*b*) A. Bhattacharyya, T. K. Ghanty, P. K. Mohapatra and V. K. Manchanda, *Inorg. Chem.*, 2011, **50**, 3913; (*c*) J. M. Keith and E. R. Batista, *Inorg. Chem.*, 2012, **51**, 13; (*d*) J. Narbutt and W. P. Oziminski, *Dalton Trans.*, 2012, **41**, 14416.
8 M. Kaneko, S. Miyashita and S. Nakashima, *Inorg. Chem.*, 2015, **54**, 7103.
9 (*a*) T. Kawasaki, S. Okumura, Y. Sasaki and Y. Ikeda, *Bull. Chem. Soc. Jpn.*, 2014, **87**, 294; (*b*) G. Tian, D. K. Shuh, C. M. Beavers and S. J. Teat, *Dalton Trans.*, 2015, **44**, 18469; (*c*) S. D. Reilly, A. J. Gaunt, B. L. Scott, G. Modolo, M. Iqbal, W. Verboom and M. J. Sarsfield, *Chem. Commun.*, 2012, **48**, 9732; (*d*) S. Kannan, M. A. Moody, C. L. Barnes and P. B. Duval, *Inorg. Chem.*, 2008, **47**, 4691.
10 (*a*) N. Yang, J. Zheng, W. Liu, N. Tang and K. Yu, *J. Mol. Struct.*, 2003, **657**, 177; (*b*) J. Zheng, N. Yang, W. Liu and K. Yu, *J. Mol. Struct.*, 2007, **873**, 89.
11 (*a*) J. H. Burns and M. D. Danford, *Inorg. Chem.*, 1969, **8**, 1780; (*b*) J. H. Burns and W. H. Baldwin, *Inorg. Chem.*,

1977, **16**, 289; (*c*) A. M. Fedosseev, M. S. Grigoriev, N. A. Budantseva, D. Guillaumont, S. Le Nauor, D. Den Auwer and P. Moisy, *C. R. Chim.*, 2010, **13**, 839.
12 F. Neese, *WIREs Comput. Mol. Sci.*, 2012, **2**, 73.
13 E. van Lenthe, E. J. Baerends and J. G. Snijders, *J. Chem. Phys.*, 1993, **89**, 4597.
14 C. van Wüllen, *J. Chem. Phys.*, 1998, **109**, 392.
15 (*a*) D. A. Pantazis, X. Chen, C. R. Landis and F. Neese, *J. Chem. Theory Comput.*, 2008, **4**, 908; (*b*) D. A. Pantazis and F. Neese, *J. Chem. Theory Comput.*, 2009, **5**, 2229; (*c*) D. A. Pantazis and F. Neese, *J. Chem. Theory Comput.*, 2011, **7**, 677.
16 (*a*) M. Kaneko, S. Miyashita and S. Nakashima, *Dalton Trans.*, 2015, **44**, 8080; (*b*) M. Kaneko, S. Miyashita and S. Nakashima, *Croat. Chem. Acta*, 2016, **88**, 347.
17 (*a*) J. Wiebke, A. Moritz, X. Cao and M. Dolg, *Phys. Chem. Chem. Phys.*, 2007, **9**, 459; (*b*) J. Ciupka, C. Cao, J. Wiebke and M. Dolg, *Phys. Chem. Chem. Phys.*, 2010, **12**, 13215.
18 (*a*) F. Neese, *J. Comput. Chem.*, 2003, **24**, 1740; (*b*) F. Neese, F. Wennmohs, A. Hansen and U. Becker, *Chem. Phys.*, 2009, **356**, 98.
19 (*a*) R. S. Mulliken, *J. Chem. Phys.*, 1955, **23**, 1833; (*b*) R. S. Mulliken, *J. Chem. Phys.*, 1955, **23**, 2338.
20 K. Momma and F. Izumi, *J. Appl. Crystallogr.*, 2008, **41**, 653.
21 M. R. Antonio, D. R. McAlister and E. P. Horwitz, *Dalton Trans.*, 2015, **44**, 515.
22 (*a*) C. Wang, J. Lan, Q. Wu, Y. Zhao, X. Wang, Z. Chai and W. Shi, *Dalton Trans.*, 2014, **43**, 8713; (*b*) J. Narbutt, A. Wodynski and M. Pecul, *Dalton Trans.*, 2015, **44**, 2657; (*c*) S. M. Ali, A. Bhattacharyya and P. K. Mohapatra, *Phys. Chem. Chem. Phys.*, 2016, **18**, 9816.
23 P. O. Löwdin, *Phys. Rev.*, 1955, **97**, 1474.
24 I. Mayer, *Chem. Phys. Lett.*, 1983, **97**, 270.
25 A. Leoncini, P. K. Mohapatra, A. Bhattacharyya, D. R. Raut, A. Sengupta, P. K. Verma, N. Tiwari, D. Bhattacharyya, S. Jha, A. M. Wouda, J. Huskens and W. Verboom, *Dalton Trans.*, 2016, **45**, 2476.
26 M. P. Jensen, R. Chiarizia, I. A. Shkrob, J. S. Ulicki, B. D. Splindler, D. J. Murphy, M. Hossain, A. Roca-Sabio, C. Platas-Iglesias, A. de Blas and T. Rodríguez-Blas, *Inorg. Chem.*, 2014, **53**, 6003.